UNIVERSITÀ DEGLI STUDI DI PADOVA


## Università degli Studi di Padova

Dipartimento di Scienze Chirurgiche, Oncologiche e Gastroenterologiche


---

CORSO DI DOTTORATO DI RICERCA IN: ONCOLOGIA CLINICA E SPERIMENTALE ED IMMUNOLOGIA - XXX° CICLO

# Decellularized colorectal cancer matrix as bioactive microenvironment for *in vitro* 3D cancer research


Tesi di dottorato redatta con il contributo finanziario di: Associazione Italiana per la Ricerca sul Cancro (AIRC); Fondazione Cassa di Risparmio di Padova e Rovigo (CARIPARO)



**Coordinatore:** Prof.ssa Paola Zanovello

**Supervisore**: Dott. Marco Agostini

**Dottorand**o: Edoardo D'Angelo

# ABSTRACT

Three-dimensional (3D) cancer models are overlooking the scientific landscape with the primary goal of bridging the gaps between two-dimensional (2D) cell cultures, animal models and clinical research. In this thesis, we describe an innovative tissue engineering approach applied to colorectal cancer (CRC) starting from decellularized human biopsies in order to generate an organotypic 3D bioactive model. This in vitro 3D system recapitulates the ultrastructural environment of native tissue as demonstrated by histology, immunohistochemistry, immunofluorescence and scanning electron microscopy analyses. Mass spectrometry of proteome and secretome confirmed a different stromal composition between decellularized healthy mucosa and CRC in terms of structural proteins (COL1A1, COL1A2, and COL3A1) and secreted proteins such as DEFA3. Importantly, we proved that our 3D acellular matrices retained their biological properties: using CAM assay, we observed a decreased angiogenic potential in decellularized CRC compared with healthy colon mucosa, caused by direct effect of DEFA3. In addition, we demonstrated that following a 5 days of recellularization with HT-29 cell line, the 3D tumor matrices induced an over-expression of IL-8, a DEFA3-mediated pathway and a mandatory chemokine in cancer growth and proliferation, compared with recellularized healthy mucosa and 2D conventional culture model. Given the biological activity maintained by the scaffolds after decellularization, we believe this approach is a powerful tool for future pre-clinical research and screenings.

# INTRODUCTION

## Colorectal Cancer: epidemiology, risk factors and classification

According to the American Cancer Society's 2017 statistics, cancer is the second leading cause of death in the world and will become the first cause of death in industrialized countries over the next two decades, overcoming cardiovascular diseases [1]. Incidence and mortality rates of Colorectal cancer (CRC) vary markedly around the world. The highest incidence rates are in Australia/New Zealand, Europe, and Northern America. Rates are low in Africa and South-Central Asia. Both incidence and mortality are higher in men than in women in most parts of the world [1].

Tumors of the gastrointestinal tract represent a serious public health problem due to the high incidence and mortality in the world population. In Europe, tumors of the gastrointestinal tract are the most common: more than half are represented by CRC, affecting about 250000 individuals per year representing 9% of all cancer diagnosed in Europe [2].

The incidence of CRC correlates with industrialization and urbanization to indicate how environmental factors together with diet and lifestyle can be considered the major risk factors. Among these of particular importance are: a diet rich in fat and meat, cigarette smoking, the use of non-steroidal anti-inflammatory drugs, alcohol, sedentary lifestyle and obesity. Conversely, a discrete contribution of folic acid, vitamins, fibers and periodic medical visits contributes to decreasing the risk of CRC [3].

CRC is a heterogeneous disease that originates from a multi-stage biological process characterized by progressive deregulation in the oncogene and oncosuppressor genes. Such genotype alterations are associated to phenotypic alterations characterized by the progressive de-differentiation of colic epithelial, the so-called “adenoma-carcinoma sequence” [4] (Figure 1).

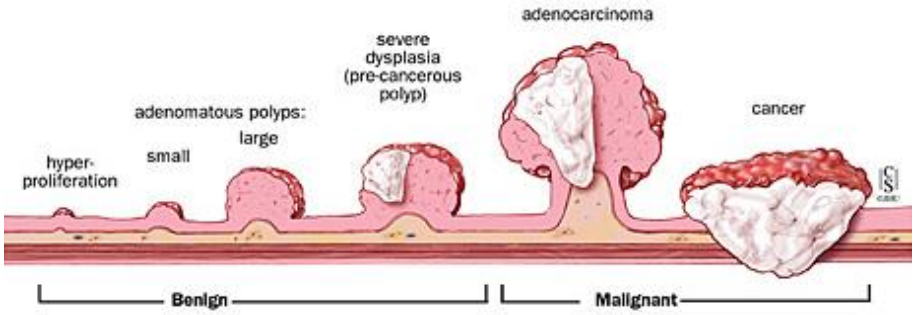


**Figure 1:** Anatomo-pathological evolution of the adenoma-carcinoma sequence.

Approximately 25% of CRCs are hereditary [5]. Among these, the most common are: Familial Adenomatous Polyposis (FAP), with abnormalities in the APC gene (Adenomatous Polyposis Coli), a dominant autosomal pathology characterized by the spread of adenomatous polyps in the colon and rectum already after the second decade of life and Lynch syndrome or Hereditary Non-polypotic Colon Cancer (HNPCC) caused by a mutation in the genes involved in the mismatch repair genes such as MLH1, MSH2 and MSH6. With lower incidence there are also Peutz-Jegher's syndrome and Juvenile polyposis both dominant autosomal pathologies characterized by the manifestation of hamartomatous polyps along the gastrointestinal tract. The remaining 75% of CRC is of sporadic origin. The acquisition of genetic instability as key event of tumor progression is to be attributed to three main genetic factors: 85% of sporadic CRCs exhibit chromosomal instability (CIN) in the form of structural or numerical anomalies of the chromosomes in the tumor cells. About 10% of sporadic CRCs are characterized by microsatellite instability (MSI), associated with the biallelic inactivation of genes involved in DNA repair. Finally, 5% of sporadic CRCs show a characteristic epigenomic instability understood both as global hypomethylation and as an alteration in methylation of the CpG (CIMP) [6].

The most common CRC classification, both sporadic and hereditary, is the TNM classification system of the American Joint Committee on Cancer (AJCC). The TNM system has been in force around the world since the mid-1980s and is based on the

evaluation of three parameters: parameter T (Tumor), indicates the degree of invasion of the intestinal wall; parameter N (Node), indicates the degree of involvement of locoregional lymph nodes; the parameter M (Metastasis), indicates the presence or absence of metastasis [7] (Table 1).

Patients with CRC stage I, II and III have 5-year Disease-Specific Survival rates (DSS rates) of 95%, 84.7% and 68.7%, respectively, and 5-year Overall Survival rates (OS rates) of 82.7%, 70.3% and 58.3%, respectively. CRCs that have spread to other parts of the body are often harder to treat and tend to have a poorer outcome. Metastatic, or stage IV colon cancers, have a 5-year OS rate of about 11% [8].

| AJCC stage | TNM classification | TNM stage criteria for colorectal cancer |
|---|---|---|
| **Stage 0** | Tis, N0, M0 | Tis: Tumor confined to mucosa; cancer-*in-situ* |
| **Stage I** | T1, N0, M0<br>T2, N0, M0 | T1: Tumor invades sub mucosa<br>T2: Tumor invades muscularis propria |
| **Stage IIA** | T3, N0, M0 | T3: Tumor invades subserosa or beyond (without other organs involved) |
| **Stage IIB** | T4a, N0, M0 | T4a: Tumor penetrates to the surface of the visceral peritoneum |
| **Stage IIC** | T4b, N0, M0 | T4b: Tumor directly invades or is adherent to other organs or structures |
| **Stage IIIA** | T1-2, N1, M0<br>T1, N2a, M0 | N1: Metastasis to 1 to 3 regional lymph nodes. |
| **Stage IIIB** | T3-4a, N1, M0<br>T2-T3, N2a, M0<br>T1-T2, N2b, M0 | N1: Metastasis to 1 to 3 regional lymph nodes. |
| **Stage IIIC** | T4a, N2, M0<br>T3-T4a, N2b, M0<br>T4b, N1-N2, M0 | N2: Metastasis to 4 or more regional lymph nodes |
| **Stage IV** | any T, any N, M1a/b | M1: Distant metastases present;<br>M1a: Metastasis confined to one organ or site;<br>M1b: Metastases in more than one organ/site or the peritoneum |

**Table 1.** TNM classification system of the AJCC, according to the "TNM Classification of Malignant Tumours, 7th Edition".

**Tumor microenvironment and extracellular matrix: the context matter**

The extensive studies on cancer, allow us to affirm that tumors arise from a normal cell following sequential gene alterations that perturb its finely tuned homeostatic system. Twenty years ago, Hanahan and Weinberg proposed the six hallmarks of cancer, the fundamental, distinctive and complementary capabilities that enable tumor growth and metastatic dissemination: sustaining proliferative signaling, evading growth suppressors, resisting cell death, enabling replicative immortality, inducing angiogenesis, and activating invasion and metastasis [9]. The scientific efforts of the researchers, in the last ten years, have made it possible a conceptual progression by adding two emerging hallmarks of cancer: reprogramming of energy metabolism and evading immune destruction. In addition, the same authors in their second publication, recognized to the tumors another grade of complexity: a repertoire of recruited normal cells that contribute to the acquisition of hallmark traits by creating permissive and promoting environment for cancer onset and progression [10].

However, the tumor cell-centric view of cancer does not take into account the context in which malignant cells subsist. As the cancer progresses, the surrounding microenvironment co-evolves into an activated state through continuous paracrine communication, creating a dynamic signaling circuitry that promotes cancer initiation and growth. A cancer is now recognized, as a complex tissue composed of multiple distinct cell types and a non-cellular compartment, within which tumor cells establish, the so-called: tumor microenvironment (TME) [11].

The TME is composed by a various stromal components, including endothelial cells, pericytes, cancer-associated fibroblasts, various classes of leukocytes, myeloid cells, and extracellular matrix (ECM) [12]. This thesis focuses its attention on the non-cellular component of TME, which is also the most abundant and less studied of the tumor niche: the ECM [13]. The ECM does not only serve as a scaffold upon which tissues are organized but provides critical biochemical and biomechanical properties that affect cell growth, survival, migration and differentiation [14]. The composition of ECM is

extremely complex and organ-specific. Usually ECM is composed by a complex network of macromolecules that assemble into three-dimensional structures and can be classified into two major types that vary in composition and structure: the pericellular matrices, in close contact with cells, and interstitial matrices, which surround cells. Basement membrane, for example, is a type of pericellular matrix, that works as interface between parenchyma and connective tissue providing an anchoring sheet-like layer for parenchymal cells. Basement membranes are principally composed of collagen type IV, laminins, nidogen 1 and 2, perlecan, agrin, collagen type XV, and collagen type XVIII [15].

Conversely, cells embedded into interstitial matrices, interact through their surface receptors, such as integrins, discoidin domain receptors and the hyaluronan receptor CD44 with a macromolecular network composed of proteoglycans, glycosamminoglicans, collagens, hyaluronic acid, secreted factors and metalloproteases. In the homeostatic processes both the cellular and extracellular components of the stroma are finely regulated and continuously remodeled by all cellular types (i.e. epithelial, fibroblasts, immune cells, endothelial cells). Biological messages received from ECM dictate cells functions and behaviors. Various growth factors, cytokines, and chemokines are deposited within ECM through binding to specific ECM molecules and are able upon well-orchestrated procedures to be released and operate at the right time in the right region. In this context, the critical aspect of the ECM is that it is dynamically remodeled and specifically tailored to the structure/function of each organ. In addition, its composition, biomechanics and anisotropy reflects the physiological state of the tissue. In fact, in the particular case of cancer onset it was demonstrated an increased deposition and an altered organization of ECM proteins similar to a fibrotic state, called desmoplasia [16].

The studies on the role of the ECM as an active component in the modulation of tumor behavior is only at the dawn, but some works have demonstrated its pro-active role in tumor development and progression. For example, patients with pancreatic cancer

show a marked stromal desmoplasia that often associates with tumor progression and poor disease outcome [17]. Similarly, expression of matrix remodeling genes such as metallo proteases (MMPs) and collagen cross-linkers is predictive of a poor prognosis for breast cancer patients [18, 19]. Fibrosis can also predispose a tissue to malignancy; patients with liver cirrhosis or cystic fibrosis, conditions that are characterized by abnormal accumulation of collagen, have an increased risk of developing cancer [20, 21]. Moreover, increased mammographic density, which associates with increased collagen deposition, correlates with an elevated risk of developing breast cancer [22]. Indeed, MMPs and high mechanical stress are predictive of tumor formation in breast cancer patients [22]. In CRC, in recent years, it has been understood that the characterization of TME is an indispensable condition for better clustering patients and identifying a tailored therapeutic approach. These findings culminated in the proposal of a new CRC classification based on the genetic profile coupled with the peculiar characteristics of TME [23]. However, there is still a large gap to be covered since all cellular components of TME have been extensively studied but, the ECM has not been studied as much in detail, even though is the most abundant part of the tumor stroma and is far from being amorphous and without biological activity.

In conclusion, the ECM regulates many of the same cellular responses that characterize the cancer hallmarks. This overlap suggests that the biochemical and biophysical properties of the ECM should be better studied using innovative approaches widely employed in other fields of science such as regenerative medicine.

**Three-dimensional colorectal cancer models**

The best experimental approach to study a highly complex pathological condition such as cancer is to comprehensively understand the mechanisms responsible for the onset, progression and diffusion. However, in such a complicated tumor microenvironment it is difficult to understand, with current technologies, the key role of biological, biochemical, biomechanical and biophysical factors that might drive human

pathophysiology in an omni-comprehensive model. The natural reaction against this challenge is to deconstruct the complex cellular microenvironment into a simpler and more predictable system. In this scenario, most of the studies has traditionally relied on two-dimensional (2D) cultures and probably much of what we know about cancer derives from the use of this experimental model. In this model, the cells grown flat and adherent as monocultures on functionalized plastic culture plates. The main advantages of this model are: *a)* cells grow easily and are easy to maintain; *b)* cells are pure and free from contaminating cells; *c)* the manipulation of cells such as induction/silencing of a protein, stimulation with biological factor and/or chemo-radiotherapeutic treatment are relatively easy; *d)* the methods for the cytotoxicity evaluation of a molecule are simple, highly standardized and repeatable and *e)* the methods of protein/RNA/DNA extraction are relatively simple [24]. However, adherent cultured cell shows clear limitations that have encouraged the development of three-dimensional (3D) models. It is now well accepted that monolayer cells do not grow in a physiological environment that leads them to assume different shapes and behaviors from what observed *in vivo*. In details, cells are forced to polarize and increase their exchange area to culture media due to the attachment to rigid and flat substrates. This led to an over-nutrition, over-oxygenation and non-reproducibility of the *in vivo* molecular gradients. In addition, in 2D setting the composition, configuration and production of ECM are significantly altered or even absent. Finally, even more evident in the anticancer treatments research, is the fact that cells can behave differently depending on their environment and on culture conditions: medium supplements, cell density, and the composition of the culture surface have a critical impact on cell proliferation, differentiation, migration, and death by affecting intracellular signal transduction leading to unpredictable reactions to exogenous stimuli [25]. Realizing that monolayer adherent culture cannot recapitulate *in vivo* native tumor complexity researchers have developed various 3D models that recapitulate certain features of solid tumor tissues, such as tumor morphology, gradient

distribution of chemical and biological factors, dynamic and reciprocal interactions/constraints between tumor and its stroma.

The addition of the third dimension to cell culture in cancer research dates back to the '70s with the seminal experiment of Sutherland et colleagues that by cultivating Chinese hamster V79 lung cells in suspension culture obtained spheroids morphologically resembling mammary carcinoma nodules [26]. From then on, a series of studies with different methods and different aims followed. In solid tumors, multicellular tumor spheroids can mimic inner avascular structure of neoplastic lesions in terms of growth kinetics, biochemical stimuli, tissue oxygenation and nutrients supply, fundamental condition completely absent in 2D culture systems. In this setting indeed, cells in the outer layer, that form a rim of 100-300 μm, are in active proliferation because they have adequate access to nutrients and oxygen, simulating *in vivo* the vascularized site of the tumor near the capillaries. While core cells show a quiescent phenotype or even form an apoptotic/necrotic core due to the limited diffusion of oxygen and nutrients, accumulation of waste and pH decreasing [27]. With these premises, Soranzo and Ingrosso et colleagues [28], growing LoVo human colon carcinoma cells using the liquid overlay technique successfully cultivated a prototype of multicellular tumor spheroids. Initially, they observed that growth kinetics was different if compared with monolayer culture. In detail, LoVo spheroids showed a doubling time of 5 days vs 37 h of monolayer cells. In addition, they observed that cell ultrastructure and organization in spheroids closely resembled those of the same cells when grown as tumors *in vivo*. Already at the beginning of the long history of 3D culture, it was understood that this system could give important information about the relationship between tumor cells and infiltrating host cells, such as fibroblast, macrophages and lymphocyte. In fact, Lees at colleagues [29] generated a multicellular tumor spheroids model of HT-29 colon cancer cells, grown *in vitro* and subsequently implanted in the peritoneal cavity of BALB/c mice. The spheroids were recovered at various time and, after dissociation, assessed for the viability by using a clonogenic assay. Little damage to spheroids was observed during

the initial four days after implantation, but more than 99% reduction in clonogenic tumor cells occurred between days four and seven. The morphological test (light and electron microscopy both *in situ* on sections and on dissociated suspensions of spheroid cells), demonstrated a correlation between spheroids damage and graft *in situ* destruction with host cell infiltration. Fascinating is the system of hybrid spheroid proposed by Lange et colleagues [30]. This system was created as prognostic assay with the potential ability to predict *in vivo* radio- and/or chemosensitivity. The hybrid spheroid assay consists on a cell suspension directly derived from tumor sample mixed in a known ratio with a suspension of clonogenicy inactivated HeLa feeder cells. By adjusting the ratio of tumor to feeder cells and by selecting the appropriate size of spheroids, the surviving fractions and survival curves of spheroids treated with both ionizing radiations and drugs can be calculated with the ratio of clonogenicity observed of treated to untreated populations. Using this method Lange et colleagues demonstrated that cells cultivated in hybrid spheroids showed a marked resistance to 5-fluorouracil, as they are *in vivo*. This resistance was not seen in monolayer culture system. The model of multicellular tumor spheroids was used by Mellor and colleagues [31] to address the clinical relevant problem of the heterogeneous population of cells in solid tumors, in which co-exist actively dividing cells accounting for only a small proportion of the total, with the remainder of the cells being in a quiescent state. Based on this, they developed a multicellular tumor spheroids model using DLD-1 human colon adenocarcinoma cells supplemented with classical complete medium called TS proliferating (high expression of Ki-67 marker) and a quiescent version cultivated in serum-starvation setup, called TS quiescent (high expression of quiescence marker p27kip1). Afterwards, the efficacy of widely used chemotherapeutic drugs was determined. Vinblastine, doxorubicin, cisplatin and 5-fluorouracil all produced significant cell death in the TS proliferating. However, while still effective, the potencies of doxorubicin and cisplatin were significantly reduced in TS quiescent. Interestingly, 5-fluorouracil and vinblastine did not produce cell death in the TS quiescent indicating that within an *in vivo* tumor subsist

micro-regions with cells that have different sensitivity to chemotherapy due to a complex ultra-structural organization. Weiswald and colleagues [32] proposed an original study in which they spontaneously obtained a 3D culture model, called Colosphere, from CRC specimens subjected to mechanical dissociation. Interestingly, they found that original tumor specimens classified as AJCC Stage III and IV showed an increased capacity to form colospheres (against AJCC Stage I and II) and this was found to be significantly correlated with tumor aggressiveness. This aggressive behavior was cancer specific because the respective healthy colon tissue failed to do so when processed in the same manner. In addition, they also demonstrated that this colospheres not only had a similar genetic pattern of the original tissue but also maintains the aggressive phenotype causing metastasis when implanted in immunocompromised mice. Recently, with the aim of creating an *in vitro* cellular culture models able to better recapitulate complex tissue architecture and mechanical stimuli, the multicellular tumor spheroid culture system was coupled with the technology of microfluidic systems integrated in bioreactors. In this fascinating scenario, Chen et colleagues [33] developed a micro-engineered platforms fabricated from PDMS using soft lithography and rapid phototyping, highly effective in generating homogenous and massive numbers of tumor spheroids with the addition advantages of body fluid flow simulation. Other advantages are the capability of generating tumor spheroids with uniform structure, possibility of long-term cultivation, and real-time imaging measurement. In this way the complexity of the experimental model increases, as there is a diffusion of nutrients and oxygen and the development of complex cell-cell junctions. However, although these experimental culture models support a 3D ultrastructural organization, it completely lacks the structural component represented by the native ECM of the tissue in which cancer cells developed and progressed and from which they are mutually influenced and which in turn reshape it over time.

**Tissue engineering applied to oncology: the decellularization process**

In order to recapitulate the 3D organization and ECM of tumors, various natural and synthetic materials were developed to provide architectural support to interacting cells [34-38]. The first and still most commonly used materials for 3D culture of cancer cells were the natural derived-ECM biomaterials such as collagen, laminin, hyaluronic acid and Matrigel®. The key properties of these compounds are: inherent cytocompatibility; intrinsic cell adhesion properties and ability to be remodeled by cells [39]. However, the batch-to-batch variability, complex molecular composition and uncontrolled degradation of these materials often make difficult to study the influence of particular properties of the ECM on tumor cells while maintaining the other variables unaltered. In parallel, to overcome the limitations of natural-derived ECM researchers have developed synthetic materials such as polyethylene glycol (PEG) and poly(lactide-co-glycolide) (PLG) that can provide more precise experimental control over biochemical and mechanical properties in modelling the tumor ECM. However, as these synthetic materials lack natural cell adhesion sites and are not readily remodeled by cells, cell adhesion ligands and biodegradable cross-linkers are often grafted to the polymers.

In the last ten years, a new model of 3D culture is affirming on the landscape of oncological research, which uses biological scaffolds derived directly from the patient to design a 3D *in vitro* culture models that mimics the structural, biochemical and biological characteristics of the native tumor. The experimental approach used to produce this 3D model is that of tissue decellularization. Decellularized tissues and organs have been successfully used in a variety of tissue engineering/regenerative medicine applications in order to replace the damaged part of the organ or the complete replacement of the impaired organ, and the decellularization methods used vary as widely as the tissues and organs of interest [40].

The term decellularization, means the removal of the cellular component of a tissue by minimally altering its biochemical composition and its biological and structural

properties. Currently, there is no precise quantitative or qualitative requirements that allow to uniquely defining the yield of a tissue decellularization. Based upon the findings of studies, the following minimal criteria are sufficient to satisfy the intent of decellularization [41]:

- <50 ng dsDNA per mg of dry weight ECM;
- <200 bp DNA fragment length of the remaining DNA;
- lack of visible nuclear material in tissue sections stained with 4',6-diamidino-2-phenylindole (DAPI) or Hematoxylin and Eosin satin.

Recently, some promising 3D tumor cell culture models have been developed and showed encouraging results in CRC research. This tissue engineering approaches, which was defined as “Tumor engineering”, are employed to study tumor cells behavior in a 3D culture model that better recapitulate the *in vivo* situation. For example, Genovese et colleagues [42] developed a decellularization protocol of matched samples of healthy colon mucosa, peritumoral tissue and CRC. They observed a complete removal of cellular compartment and the maintenance of the main structural components of colonic mucosa, healthy and CRC, as well as the proper proteins distribution along the tissue. In addition, they developed a recellularization protocol for repopulating decellularized mucosa with stabilized CRC lines that demonstrated the ability to grow and invade the acellular patients-derived scaffolds.

Another recent work of Pinto et colleagues [43], revealed the relationship between macrophages and ECM and the ability of the latter to influence macrophage polarization in a physiological environment compared to the CRC. Notably, in this study, healthy colonic mucosa and CRC were decellularized and characterized for their biochemical and mechanical properties. Afterwards, they repopulated decellularized healthy mucosa and CRC with human isolated macrophages in order to evaluate whether normal and tumor-decellularized matrices had the ability to differently modulate macrophage polarization, in terms of gene expression and secretion of pro- and anti-inflammatory

cytokine and chemokine. Interestingly, they showed that normal and tumor decellularized ECM distinctly promoted macrophage polarization, with macrophages seeded in tumor matrices differentiating towards an anti-inflammatory M2-like phenotype. In addition, using an invasion assays they revealed that tumor ECM-educated macrophages stimulated cancer cell invasion through a mechanism involving CCL18.

## PURPOSE OF THE THESIS

The PhD project that I carried out during these three years had the following aims:

a) To standardize a decellularization protocol for the healthy colonic ECM and CRC counterpart, able to eliminate the cellular component but simultaneously maintainings its structure, biochemical composition and biological properties;

b) To characterize the decellularized healthy and CRC ECM by analyzing the main structural components, its three-dimensional organization and the proteome and secretome composition;

c) To verify whether the CRC ECM possesses different biological properties compared with healthy colonic mucosa by means of recellularization experiments with stabilized CRC cell lines.

## MATHERIAL AND METHODS

### Patients

A series of 28 paired normal mucosa (N) and cancer lesion (T) tissue samples from CRC patients who underwent curative surgery between February 2015 and December 2016 were collected from First surgery clinic, Surgery Unit at the University of Padua (Department of Surgery, Oncology and Gastroenterology) and General Surgery Unit, S. Antonio Hospital (Padua). This study was conducted according to the principles expressed in the Declaration of Helsinki. Written informed consent was obtained from every enrolled individual and ethics committee of institution approved the protocol. All of the patients enrolled fulfilled the following inclusion criteria: histologically confirmed primary adenocarcinoma of the colon, age > 18 years, and written informed consent. Patients with a known history of a hereditary colorectal cancer syndrome and patient that underwent neoadjuvant treatments were excluded (Table 2).

| | | **Total (N=28)** |
|---|---|---|
| **Median age (interval)** | | 72.5 (39-87) |
| **Sex** | Male<br>Female | 17 (60,7%)<br>11 (39,3%) |
| **Grading** | G1<br>G2<br>G3 | 2 (7%)<br>19 (68%)<br>7 (25%) |
| **Staging** | I<br>II<br>III<br>IV | 4 (14.3%)<br>11 (39,3%)<br>9 (32,1%)<br>4 (14,3%) |
| **Type of surgical** | Sigmoidectomy<br>Hemolectomy right<br>Hemolectomy left<br>Abdominoperineal resection of rectum | 6 (21%)<br>10 (36%)<br>7 (25%)<br>5 (18%) |

**Table 2.** Clinical and pathological characteristics of N=28 colorectal cancer patients enrolled in the study.

**Tissue decellularization**

All mucosa specimens encompassed the luminal surface, mucosa and submucosa. CRC tissue was obtained at the edge of infiltrating neoplasia and matched healthy colon mucosa was obtained more than 10 cm far from the cancer lesion. Surgically obtained healthy mucosa and CRC specimens were kept in cold and sterile phosphate buffered saline (PBS) for no longer than 2 h before processing. All the decellularization steps were performed with sterile solutions and under tissue culture hood. Healthy mucosa and CRC destined to be used as fresh samples (FN= fresh normal tissue; FT= fresh tumor tissue) were rinsed with sterile PBS and consequently treated according to the methodology with which were analyzed. Healthy mucosa and CRC destined to decellularization process (DN= decellularized normal tissue; DT= decellularized tumor tissue) were treated with one to three detergent-enzymatic treatment (DET) cycles. Each DET cycle was composed of deionised water at 4 °C for 24 h, 4 % sodium deoxycholate (Sigma) at room temperature (RT) for 4 h, and 2000 kU DNase-I (Sigma) in 1 M NaCl (Sigma) at RT for 3 h, after washing in water. After decellularization, matrices were rinsed in PBS +3 % penicillin/streptomycin (pen/strep) for at least 5 days changing the solution two times a day and then stored at -80 °C.

**DNA isolation and quantification**

To assess total DNA content within the fresh healthy mucosa and CRC compared with decellularized matrices, 20 mg of each specimen were treated using DNeasyBlood&Tissue kit (Qiagen) under manufacturer's instruction. DNA samples were then quantified using Nanodrop 2000 spectrophotometer at 260/280 nm ratio (Thermo Scientific, USA). Agarose gel (1 %, containing 1 % SYBRsafe) was used to separate DNA and bands were visualized by exposing the gel to UV light and images acquired by Gel Doc (Biorad). Fresh and decellularized specimens were loaded into the gel, and DNA ladder of lambda DNA were used as controls.

**Immunohistochemistry and immunofluorescence**

Frozen sections (8 µm thick) were stained with Haematoxylin & Eosin (HE; Bio Optica, Milan, Italy), Masson trichrome (aniline blue kit; Bio Optica), Alcian blue stain (pH 2.5 kit; Bio Optica) and Van Gieson trichrome (Bio Optica) for elastic fibers and connective tissue, Silver Stain (Bio Optica), Periodic Acid Schiff (PAS; Bio Optica), anti-collagen IV [1:100, Dako, Milan, Italy], and anti-Defensin alpha 3 antibody - C-terminal (1:100, Abcam, Cambridge, UK). All the stainings were performed according to manufacturer's instruction. Immunohistochemical (IHC) stainings were automatically performed using the Bond Polymer Refine Detection kit (Leica Biosystems, Newcastle upon Tyne, UK) in the BOND-MAX system (Leica Biosystems).

For immunofluorescence analysis, sections were permealised with 0.5 % Triton X-100, blocked with 10 % horse serum and incubated with primary antibodies [Laminin (1:100, L-9393 Sigma); Ki-67 (1:100, ab15580 Abcam)], then slides were washed and incubated with labelled Alexa Fluor secondary antibodies. Finally, nuclei were counterstained with fluorescent mounting medium plus 100 ng/mL 40,6-diamidino-2-phenylindole (DAPI) (Sigma-Aldrich). For each specimen, random pictures were collected with a direct microscope.

**ECM component quantification**

Collagen and sulphated glycosaminoglycan (sGAG) content on fresh and decellularized healthy mucosa and CRC were quantified using respectively the SIRCOL collagen assay and Blyscan GAG Assay Kit (all from Biocolor, UK) under manufacturer's instruction.

**Scanning electron microscopy (SEM)**

Samples were fixed with 2 % glutaraldehyde in 0.1 M phosphate; following washing they were cut into segments of approximately 1 cm length and cryoprotected in 25 % sucrose, 10 % glycerol in 0.05 MPBS (pH 7.4) for 2 h, then fast frozen. At the time of

analysis, samples were placed back into the cryoprotectant at RT and allowed to thaw. After washing, the material was fixed in 1 % $OsO_4$/0.1 M phosphate buffer (pH 7.3) and washed again. After rinsing with deionized water, specimens were dehydrated in a graded ethanol-water series to 100 % ethanol, critical point dried using $CO_2$ and finally mounted on aluminum stubs using sticky carbon taps. Samples were mounted and coated with a thin layer of Au/Pd (approximately 2 nm thick) using a Gatan ion beam coater. Images were recorded with a Jeol 7401 FEG scanning electron microscope.

**Mass Spectrometry analysis**

Paired normal mucosa/tumor tissues (average weight 33.8 mg) were decellularized and analyzed by mass spectrometry as follow.

*Samples preparation*

Normal/tumor tissue secretome was collected by implementing the original procedure proposed by de Wit et al. (23) with a sequential extraction procedure. Briefly, decellularized samples were cut to 1 $mm^3$ pieces and placed in 50 mM ammonium bicarbonate buffer at 4 °C for 1 h to collect low-bind proteins of secretome. Surnatant (fraction A) was removed and concentrated onto 30 kDa MWCO centrifugal filters (Amicon Ultra, Millipore). A second extraction of decellularized ECM was performed in presence of 7 M urea, 20 mM dithiothreitol (DTT), 0.5 % SDS in 50 mM ammonium bicarbonate (1h at 56 °C) to recover cross-linked secreted proteins within the matrix. All reagent were of highest purity available from Sigma-Aldrich. Surnatant (fraction B) was removed and concentrated onto 30 kDa MWCO centrifugal filters. Fractions A and B were reduced (20 mM DTT, 1h at 56 °C) and alkylated (50 mM iodoacetamide (IAA) 30 mins, in the dark) and then digested with trypsin (final protein to trypsin ratio 1:50). The remaining decellularized ECM was then treated with 50 mM of IAA in ammonium carbonate (30 mins, in the dark) and finally dehydrated with 0.25 mL of acetonitrile before performing the in-matrix digestion of residual insoluble proteins. Dehydrated

ECM samples were digested overnight at 37 °C in presence of a 100 µg/mL trypsin solution (Sequencing Grade Modified Trypsin PROMEGA) added to the completely re-hydrate the ECM pieces. After digestion, samples were centrifuged (14000 rpm, 30 min at 4 °C) to collect surnatant (fraction C). The extraction performances in terms of reproducibility, specificity and efficacy have been evaluated in the sequential extraction of two independent samples of healthy human colonic mucosa (data not shown).

*MALDI-TOF and MALDI-TOF/TOF analysis*

Mass spectra of digested peptides were acquired using an Ultraflex II TOF/ TOF (Bruker Daltonics, Bremen, Germany) instrument equipped with an Nd:YAG laser (λ 355 nm) and operating in reflectron positive ion mode in the mass range 500-4000 m/z. External mass calibration was based on the monoisotopic values of peptides present in the Peptide Calibration Standard II (Bruker Daltonics, Bremen, Germany). Before deposition onto the MALDI plate, samples were desalted with ZipTipC18 (Millipore, Darmstadt, Germany) following the manufacturer instruction; purified peptides were eluted in 1 µl of α-CHCA saturated solution in 50 % acetonitrile and 0.1 % trifluoroacetic acid. mMass open source software was employed for spectra alignment, denoising (precision 15, relative offset 25, arbitrary units) and smoothing (Savitzky–Golay filtering, m/z 0.15) before manual peak picking (threshold set S/N> 6) and intensity normalization following the TIC (Total Ion Count) procedure.

Tandem mass spectra were subjected to Mascot search engine (Matrix Science, London, UK) for proteins identification. Search parameters were set as follow: database, Swiss-prot; enzyme, typsin; taxonomy, Homo sapiens; precursor ions tolerance, 0.2 Da, MS/MS fragments tolerance, 0.8 Da; fixed modification: carbamidomethyl (C); variable modifications: oxidation (H,M,P,K), deamidation (N,Q), amidation (C terminal), phosphorylation (ST), and acetylation (K, N terminal).

**Chicken chorioallantoic membrane assay**

Chicken chorioallantoic membrane (CAM) assay was used as previously described [44]. Fertilized chicken eggs (Henry Stewart and Co.) were incubated at 37 °C and constant humidity. At 3 days of incubation, an oval window of approximately 3 cm in diameter was cut into the shell with small dissecting scissors to reveal the embryo and CAM vessels. The window was sealed with tape and the eggs were returned to the incubator for a further 5 days. At day 8 of incubation, 1 mm diameter acellular matrices were placed on the CAM between branches of the blood vessels. Polyester sections soaked overnight either in a PBS solution or in PBS with 200 ng/mL VEGF were used as negative and positive controls, respectively. Samples were examined daily until 10 days after placement wherein they were photographed *in ovo* with a stereomicroscope equipped with a Camera System (Leica) to quantify the blood vessels surrounding the matrices. The number of blood vessels (less than 10 µm in diameter) converging towards the placed tissues was counted blindly by n=4 assessors, with the mean of the counts being considered.

**ELISA test**

The concentration of alpha Defensin 3 in fresh and decellularized (healthy colon mucosa and CRC) tissue samples was measured using commercially available ELISA kit, according to the manufacturer' instructions (Human DEFA3/Defensin Alpha 3 ELISA Kit (Sandwich ELISA) - LS-F6599, LifeSpan Biosciences, Inc).

**RNA extraction and qRT-PCR**

In the *in vitro* experiments, total RNA was extracted using RNeasy Mini Kit (Qiagen), according to the manufacturer's instructions. In the recelullarized sample, total RNA was extracted using TissueLyser (Qiagen) combined with Trizol, according to the manufacturer's instructions. The concentration and purity of the RNA were determined by NanoDrop 2000 spectrophotometer (Thermo Scientific, USA). The quality of RNA

was considered to meet the requirements if the Optical Density (OD) ratio at 260 nm/280 nm was between 1.7 and 2.1.

cDNA was synthesized from 500 ng of total RNA using the High-Capacity cDNA Reverse Transcription Kit (Applied Biosystems, Foster City, CA, USA), according to the manufacturer's protocol by the Veriti™ 96-well Thermal Cycler instrument. qPCR was performed using the 7500 Fast Real-Time PCR System (Applied Biosystems) with HPRT1 gene as endogenous control (Assay ID: Hs99999909_m1). The amplification reaction was conducted in a final volume of 20 µl using 4 µl of cDNA, TaqMan® Universal PCR Master Mix 1X (Applied Biosystems) and specific TaqMan® Gene Expression Assay 1X (Applied Biosystems): Hs00174103_m1 (amplicon length 101 bp) for CXCL-8 or *IL-8*. The thermal conditions included one cycle at 50 °C for 2 mins for the UNG incubation and at 95 °C for 10 mins for the polymerase activation, followed by 40 cycles at 95 °C for 15 s for denaturation and at 60 °C for 1 min for annealing and extension. Each sample was run in duplicate and the threshold cycle (Ct) average was used for the calculations. The results from each sample were compared with one cDNA sample as calibrator, using the $2^{-\Delta\Delta Ct}$ calculation method. The fold change was expressed as Relative Quantification (RQ).

**In vitro experiments**

*Conditioned Medium Assay*

The human colon adenocarcinoma cell line HT-29 was obtained from American Type Culture Collection (ATCC) and maintained in RPMI-1640 medium supplemented with 10 % fetal bovine serum, 1 % L-Glutamine and 1 % Penicillin/Streptomycin antibiotic solution (Growth medium, [GM]) in humidified atmosphere at 37 °C in 5 % $CO_2$. For the preparation of Conditioned Medium (CM), 150 mg of fresh/DET normal/CRC samples were disaggregated in 1 mL of GM using TissueLyser (Qiagen) equipped with 7 mm stainless steel beads (two cycles, 2 min each at 30 Hz). HT-29 cells were seeded at a density of $4x10^4$ cells/well in a 24-well plate tissue culture and incubated at 37 °C in 5

% $CO_2$ for 24 h. After 24 h, GM was collected and replaced with CM (control wells were replaced with GM). After 48 h of incubation, cells were detached using 0.025 % trypsin for 5 min at 37 °C and RNA was collected as specified above for downstream analysis.

*In vitro Migration Assay*

HT-29 cells ($4x10^4$ cells/well) were plated on uncoated upper chambers (24-well inserts; pore size, 8 µm; Sarstedt) for trans-well migration assay. The medium in the top component was replaced with conventional GM 12 h after seeding. At the lower compartment, DN and DT matrices were added. Cells were allowed to migrate for 24 h, and then the cells on both sides of the chamber were fixed with 4 % PFA for 5 min at RT and permeabilized with 100 % methanol for 20 min. Cells at the bottom of the chamber were stained with Mayer Acid Emallume. Then, picture of each well was taken and cell nuclei in each field was counted using Image-J software.

*Acellular matrices recellularization*

Match DN and DT matrices were washed with PBS and incubated overnight with RPMI-1640 medium supplemented with 10 % fetal bovine serum, 1 % L-glutamine and 1 % Penicillin/streptomycin antibiotic solution at 4 °C. Before repopulation, in order to normalize intra-sample variability, DN and DT matrices were cut with a 5 mm diameter stainless steel puncher (Kai Medical). Normal and tumor-derived matrices were then transferred into a 6-well plate and fixed to an agarose support with pins. Subsequently, $1x10^6$ HT-29 cells were resuspended in 15 µL of Matrigel (diluted 1:10 with RPMI-1640), carefully placed over the sample and incubated for 3.5 h in humidified atmosphere at 37 °C in 5 % $CO_2$. Finally, conventional growth medium was carefully added and changed every 2 days. HT-29 cells were cultured in 3D acellular matrices for 5 days. For each matched samples, recellularization experiments were performed in double. For the creation of a 3D synthetic environment, HT-29 cells were cultured in HyStem® Hydrogels kit; it's includes Thiol-modified sodium hyaluronate (HyStem®), Thiol-

reactive PEGDA crosslinker (Extralink®), Thiol-modified collagen (Gelin-S®) and deionized water (DG Water). HT-29 cells ($1x10^6$ cells) have been encapsulated in a solution mix (Gelin-S and HyStem) in a 1:1 volume ratio into a 24 well plate and after 30 min added Extralink. Gel was incubated for 3 h in humidified atmosphere at 37 °C in 5 % CO2. Finally, conventional growth medium was carefully added. HT-29 cells were cultured in HyStem® Hydrogels for 5 days with or without exogenous DEFA3 (5ng/mL).

**Sample analyses and distribution**

Collected samples were divided into the experimental tests as follows: setting-up of decellularization protocol and DNA content evaluation: n=3 matched samples. Immunohistochemestry and Immunofluorescence: n=4 matched samples. Collagen and GAGs quantification: n=6 matched samples. Scanning electron microscopy analysis: n=3 matched samples. Mass Spectrometry analysis: n=3 matched samples were used to set-up the experimental conditions of sample preparation and analysis, experimental data were generated by analyzing n=5 matched sample. CAM assay: n=6 matched samples. ELISA test for DEFA3 quantification: n=11 matched sample. Conditioned medium assay: n=6 matched samples. *In vitro* Migration Assay: n=5 matched samples. Acellular matrices recellularization: n=4 matched samples. A total of n=56 matched sample were collected and employed from 28 patients enrolled in the study.

**Statistical analyses**

All graphs and statistical analysis were performed using GraphPad Prism Software v.5. Data are expressed as means ± SEM. For comparison between experimental and control group two-sided Student's *t*-tests (for parametric dataset) and Mann-Whitney test (for non-parametric dataset) were used. One-way ANOVA with Bonferroni's post-test (for parametric dataset) and Kruskal-Wallis test with Dunns post-test (for non-parametric dataset), was performed for multiple comparisons. A p-value $<0.05$ was

considered statistically significant (*: p-value <0.05; **: p-value <0.01; ***: p-value <0.001).

# RESULTS

## Decellularization efficiency

Matched samples from both normal (non-neoplastic, N) and tumor (T) specimens were decellularized using detergent-enzymatic treatment (DET). After each cycle, DNA amount was quantified in order to find the best cycle number in terms of nuclei depletion and genetic material removal. Both N and T samples were completely decellularized after 2 DET cycles with a reduction of 96.26 % and 94.35 %, respectively (p-value= 0.0033 and p-value= 0.015, Figure 2A,B and Supplementary figure 1). At first, a general overview of tissue architecture maintenance was performed through HE, van Gieson and Silver stains, in order to characterize the decellularized samples (DN = decellularized normal tissue, DT = decellularized tumor tissue; Figure 2C). As underlined by histology, decellularized samples preserved the structure and the main protein composition that resulted similar to the fresh tissues (FN = fresh normal tissue; FT = fresh tumor tissue; Figure 2C). Moreover, SEM analysis confirmed the ultrastructure maintenance also after decellularization process (Figure 2D).

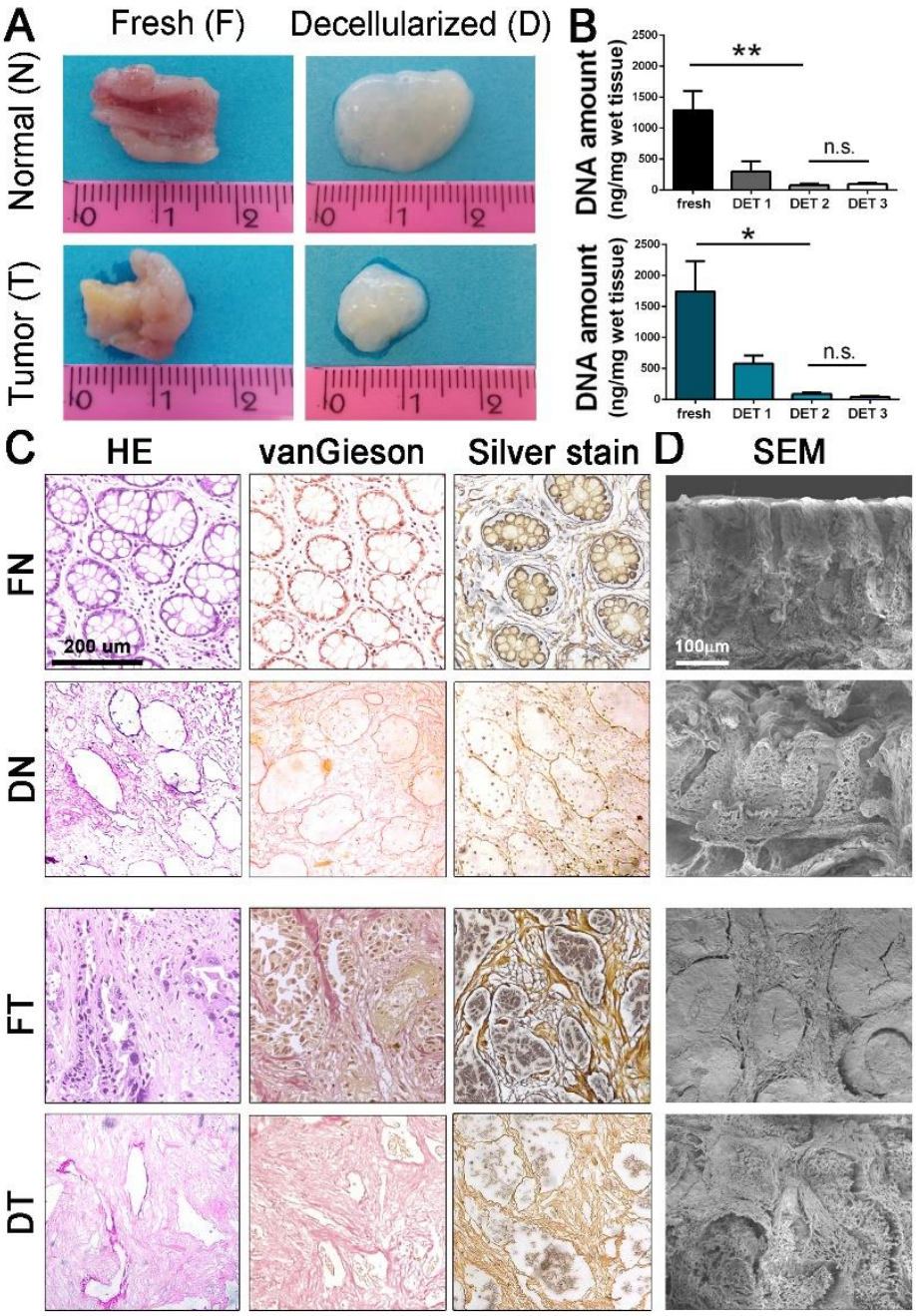


**Figure 2: Decellularization efficiency. (A)** Gross appearance of normal healthy mucosa (N) and tumor (T) biopsies before and after 2 cycles of decellularization. **(B)** DNA amount quantification of N and T samples after different detergent enzymatic treatment (DET). **(C)** Fresh (FN and FT) and decellularized (DN and DT) samples histologies. **(D)** Scanning electron microscopy of fresh and decellularized biopsies.

**Decellularized tissue characterization**

As second step, we characterized through histology and protein quantification the DN and DT matrices composition. Despite MT and collagen IV stains showed the presence of collagens in fresh and decellularized tissues with maintenance of distribution pattern, protein quantification highlighted a decrease of total collagens in decellularized samples with respect to the fresh counterparts (87.28 % of protein loss in DN, p-value=0.025 and 79.5 % in DT, p-value= 0.0141; Figure 3A,C). About the latter, our histological results are consistent with literature findings in which an increase of collagen cross-linking in tumor is reported [45-47]. Therefore, the enzymatic treatment we used through pepsin digestion for the precipitation and quantification of collagens was more efficient in FN respect to FT samples probably due to the less proportion of cross-linking. Moreover, it is evident that non cross-linked collagens are more sensitive to our decellularization protocol in respect to those are cross-linked, leading to a slightly greater loss of collagens in the healthy tissue than in tumor. This discrepancy between histology and protein quantification was partially confirmed also after GAG analysis. Indeed, AB and PAS stains evidenced the presence of GAG in both fresh and decellularized tissues, but quantification of sulphated GAG was quite different between N and T samples: a significant decrease in protein quantity was found in DN in respect to FN (p-value=0.03; 71.35 % of protein loss), whereas no meaningful differences were found between DT and FT (p-value=0.19; 60 %; Figure 3B,D). Importantly, immunostaining for laminin, another major ECM component, clearly demonstrated that after DET this glycoprotein is uniformly distributed through the decellularized samples and the immunostaining confirmed the preservation of ordered and physiological villi in DN and at the same time a disorganized and unstructured tissue in DT (Figure 3E).

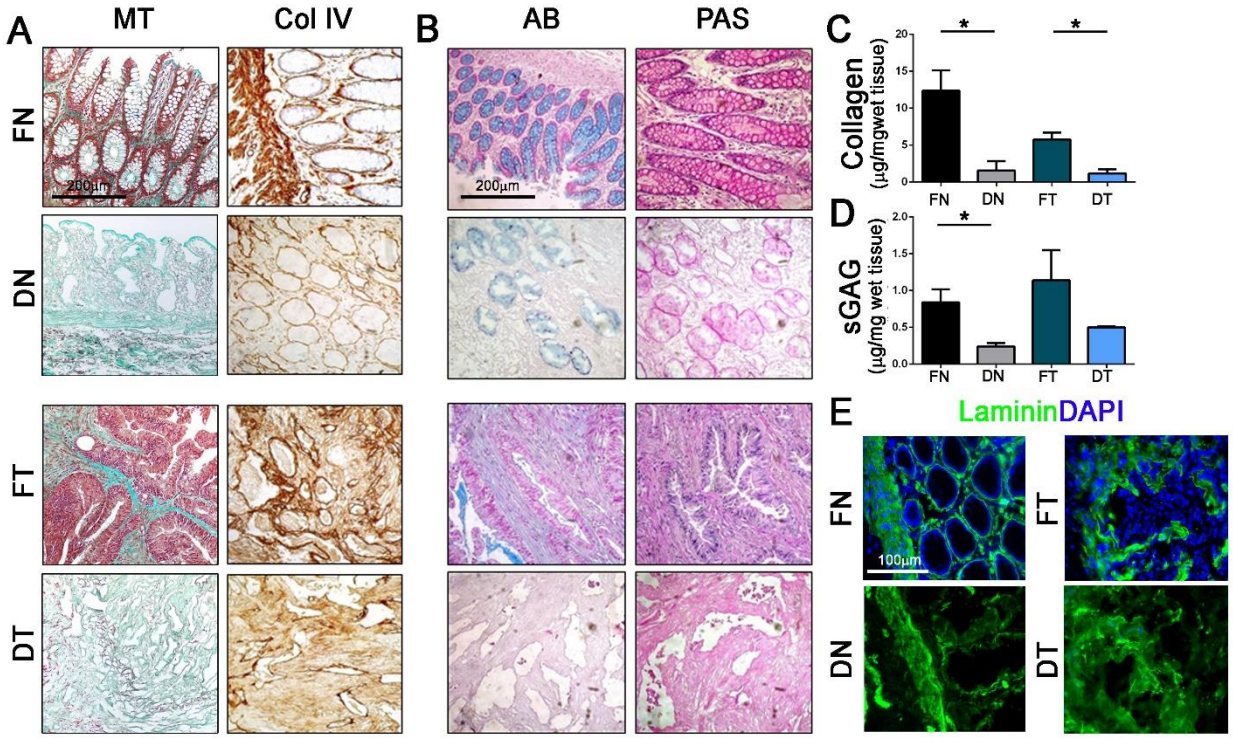


**Figure 3: Decellularized tissue characterization. (A)** Masson's Trichrome (MT) and collagen IV (Col IV) stains for the detection of collagens in fresh and decellularized samples. **(B)** Alcian blue (AB) and periodic acid–Schiff (PAS) stains for the detection of polysaccharides, glycoproteins and glycolipids in fresh and decellularized samples. **(C-D)** Quantification of collagens (I to V) and sulphated glycosaminoglycans (sGAG) in fresh and decellularized samples. **(E)** Immunofluoresence of Laminin in fresh and decellularized samples. Nuclei are counterstained with DAPI.

### Proteomic analyses of decellularized tissue secretome and migration assay

To better analyze tissue protein maintenance also after decellularization process, a mass spectrometry analysis was performed. By MALDI-TOF/TOF analysis, a total of 71 non redundant proteins were identified in the three collected fractions (fraction A, B, and C) of decellularized samples (Table 3). The sequential extraction procedure has been developed to collect low-bind secreted proteins (fraction A), cross-linked within the matrix secreted proteins (fraction B) and residual insoluble secreted proteins (fraction C). This procedure ensured a good reproducibility (CV % in two independent sample extraction procedures < 3 %) and a strong selectivity in the collect unique ionic species (m/z) in the three fractions (data not shown). Identified proteins were then classified on the basis of their predicted localization following the ProteinAtlas database classification

(http://www.proteinatlas.org/). Venn diagram reported in Figure 4A shows the predicted distribution of identified proteins in decellularized tissues.

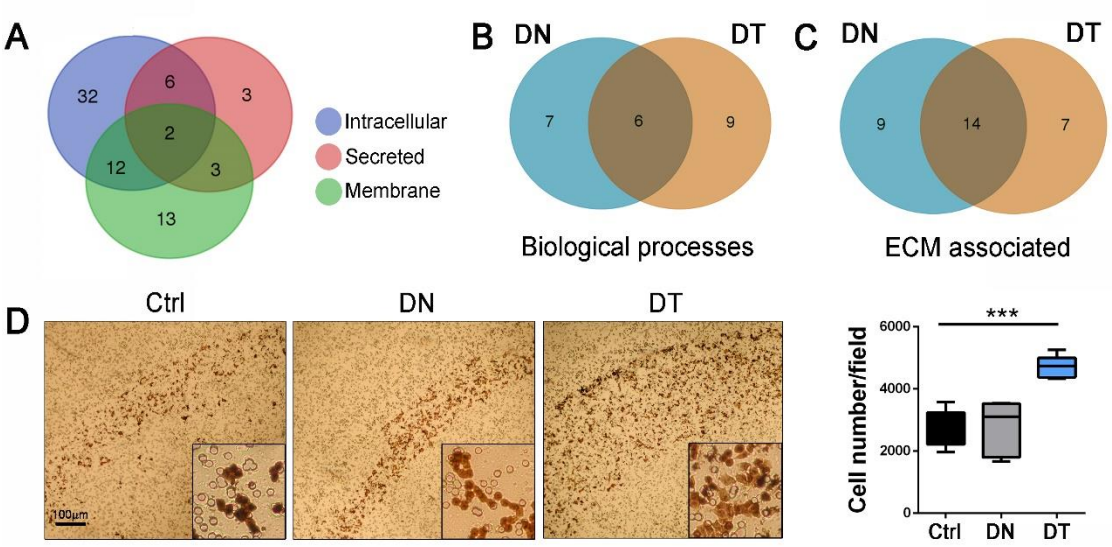


**Figure 4: Proteomic analyses of decellularized tissue secretome and migration assay. (A)** Venn diagram showing the predicted localization of proteins detected in decellularized samples. **(B-C)** Comparison of detected protein abundance in decellularized healthy tissue (DN) vs tumor tissue (DT). **(D)** Invasion assay: representative images of HT-29 cell migration after incubation medium only (Ctrl), DN and DT samples. Graph shows the number of cells per field that migrated through the trans -well in each type of sample (counts were made in blind by 2 operators).

As expected, most of detected proteins were predicted to be secreted, whereas several others were predicted to be intracellular with the actin-related proteins and myosins as the most representative groups. We hypothesized that observed signals were related only to residual proteins fragments trapped into the matrix by covalent (i.e. sulphur bridges) or non-covalent (i.e. Van der Waals or hydrophobic) interactions.

We then compared the relative abundance of detected proteins to identify key components in DT with respect to the DN counterpart. A peak list (m/z, intensity) was obtained from the full scan mass spectra of collected fractions from ECM. Obtained peaks were filtered based on frequency criteria and only peaks observed in 60 % of samples (i.e. at least in 3 out of 5 analyzed samples) were retained. A threshold in the tumor to normal mucosa ratio of 1.5 fold change has been considered to select those proteins characteristics of tumor tissue (Table 3) and all the proteins presenting a < 0.6 fold change were considered characteristics of normal tissue.

| Common proteins | Normal tissue proteins (< 0.6 fold change) | Tumor tissue proteins (> 1.5 fold change) |
|---|---|---|
| ADAM10 | PCDH11Y | AMER3 |
| ADAM22 | C6 | COL1A1 |
| AMOTL2 | CD55 | COL1A2 |
| BACE1 | COL6A2 | COL3A1 |
| CASP10 | COLGALT2 | DEFA3 |
| COL5A1 | DES | EMCN |
| COL6A1 | EFEMP1 | EPX |
| COL6A3 | FBN1 | FGA |
| COL6A6 | HSPB1 | FGB |
| COL8A2 | HSPG2 | HIF1A |
| DMKN | PCDH18 | MMP24 |
| FLNA | PCDHGC5 | PCDHGC4 |
| HIF1AN | PITPNM1 | PLEKHG5 |
| HIST1H2B | SIGLEC1 | PRG2 |
| HIST1H2B | TAGLN | PRRT2 |
| HSPB6 | TNC | STOML2 |
| KRT1 | TPM2 | TNS4 |
| LAMA3 | TRAM1 | |
| LAMB4 | VIM | |
| LGALS1 | | |
| LGALS7 | | |
| MXRA5 | | |
| MYL11 | | |
| PLEKHA5 | | |
| PRRT4 | | |

**Table 3:** List of identified proteins and their relative abundance in normal and tumor tissues.

All the detected proteins were divided on the basis of their activity or field of action. Among those involved in biological processes, we identified 22 total proteins 6 of which were equally present in the analyzed samples, 7 more present in the DN and 9 more present in the DT (Figure 4B). About ECM and ECM-related protein, we found 30 total proteins, of which 14 equally present between DN and DT, 9 more present in healthy tissue and 7 more present in tumor samples (Figure 4C). Since among all the detected proteins, there were also those responsible or involved in cell attraction and migration such as STOML2 and TNS4 [48, 49] and relying on previous works, in which acellular scaffold showed to be able to induce cell invasion [50, 51], we decided to evaluate the impact of DN and DT samples on cell migration. Accordingly, HT-29 cells were attracted with DN and DT matrices using an *in vitro* transwell-based invasion assay. We observed

that decellularized matrices were able to attract a greater cell amount in respect to the control (only medium; Figure 4D), and that invasion ability of HT-29 cells with DT samples was significantly increased in respect to cells conditioned with DN (p-value= 0.0006; Figure 4D), confirming what found previously with proteomic analysis in which STOML and TNS4 were found more abundant in tumor samples. This result demonstrated the ability of the acellular matrices to release soluble factors retained after decellularization and support the data obtained by proteomic analysis.

**Decellularized tissue biologic activity**

To test the bioactivity of DN and DT samples in relation to the peptides retained in the ECM also after the decellularization process, we analyzed the effect of a representative factor, DEFA3 that was found significantly more abundant in tumor samples after proteomic analysis. To confirm the presence of DEFA3, we performed ELISA test and immunostaining to detect and localize the protein inside the matrices (Figure 5A,B). It is known in literature that DEFA3, a human neutrophil peptide with antibiotic activity and abundantly secreted upon neutrophil activation, possess anti-angiogenic properties [52]. We verify the angiogenic activity of our decellularized matrices using CAM assay, a standard *in vivo* test: 10 days after *in ovo* samples application, DT specimens were able to attract significant less vessels and capillaries in respect to DN samples (p-value= 0.0066; Figure 5C). Moreover, it is reported that the stimulation of tumor cell lines with DEFA3 resulted in the induction of *IL-8* overexpression [53, 54]. Also in our hands, stimulation of HT-29 cell line with exogenous administration of DEFA3 (Figure 5D) or CM obtained through DN and DT matrices disaggregation (Figure 5E) induced the overexpression of *IL-8* in respect to the untreated cells (Figure 5D,E), even though this expression was not significantly different between DN and DT conditioned cells. Importantly, HT-29 cells seeded over DN and DT patient-derived matrices and let to colonize and partially repopulate the 3D environment for 5 days, as indicated by HE and staining for the proliferation marker KI67 (Figure 5F), showed a significant

overexpression of *IL-8* transcript in DT compared with DN samples (p-value=0.004; Figure 5G). This property seems to be related to the synergic effect of 3D acellular matrix conformation and DEFA3 spatial availability given that HT-29 cells cultivated in 3D inert gel did not overexpressed *IL-8*, neither when proportional concentration of DEFA3 was added to the culture medium (Figure 5G). Taken together this data indicate that our decellularized patient-derived matrix not only maintains unaltered its physical and structural properties but also has pro-active biological features, based on the original characteristics.

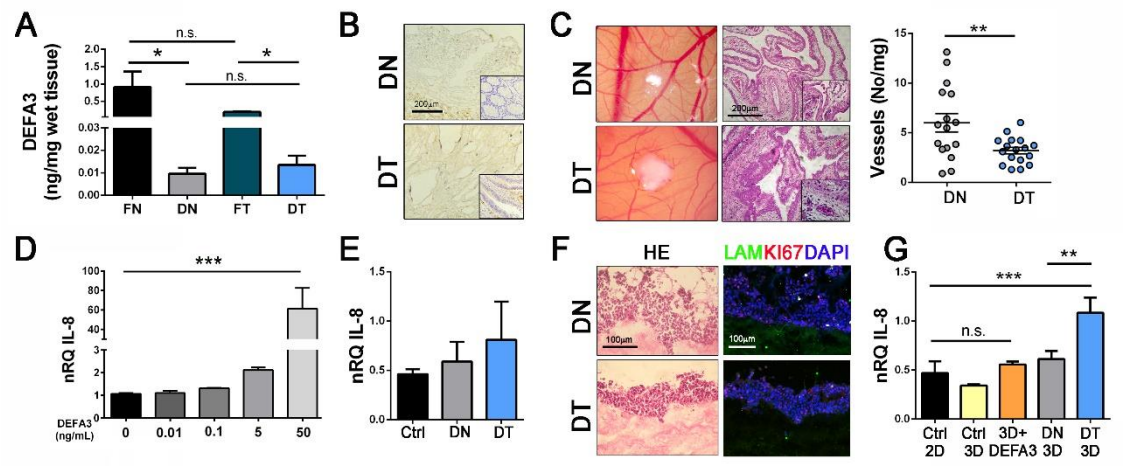


**Figure 5: Decellularized tissue biologic activity. (A)** ELISA test for the detection of DEFA3 in fresh and decellularized samples from both healthy mucosa and tumors. **(B)** Anti-DEFA3 immunostaining in DN and DT biopsies (insert: fresh tissues). **(C)** CAM assay: gross appearance after 10 days of of *in ovo* samples application and HE staining of the collected samples. Graph shows the quantification of attracted chicken vessels and capillaries. Counts were performed in blind by 4 operators. **(D)** Expression of *IL-8* transcript after increasing administration of DEFA3 in HT-29 cells. **(E)** Expression of *IL-8* transcript by HT-29 cells culture in basal medium (Ctrl), or conditioned medium obtained after mechanical disaggregation of decellularized healthy tissue (DN) and tumor tissue (DT). **(F)** Histological appearance of representative 5 days 3D culture of HT-29 cells with DN and DT samples. Haematoxylin and Eosin (HE), Immunofluoresence with Laminin (green), KI67 (red) and nuclei (blue). **(G)** Expression of IL-8 transcript by HT-29 cells after 5 days of 3D culture over inert gel (HyStem® Hydrogels) with or without exogenous DEFA3 (5ng/mL), DN (DN 3D) or DT (DT 3D) samples. Cells cultured on 2D plastic dishes were used as controls (Ctrl 2D).

# DISCUSSION

In this thesis, we demonstrated that decellularization is a valid approach to obtain an *in vitro* 3D microenvironment from healthy colon mucosa and CRC specimens that maintains peculiar biological activity depending on the original physiological or pathological condition.

Genetic alterations impairing the tightly controlled systems of cellular homeostasis are responsible for the onset of CRC. Despite the important knowledge derived from genetic analyses and the discovery of relationship among mutations and tumor progression, less is known about the role of cell and tissue microenvironment interaction in cancer development. In the last decade, the cancer cell-centric view has been flanked by the tumor microenvironment concept. In this context, the most abundant component of tumor microenvironment is the ECM that provides critical biochemical and biophysical properties influencing cell differentiation, polarity, growth, survival, proliferation and fate. Although this idea is being established, at present there are no 3D culture models able to provide the correct *in vitro* mechanical and biochemical stimuli to be used as reliable assays in pre-clinical studies.

In this scenario, we propose a tissue decellularization method that allows achieving excellent nuclei depletion preserving ECM components starting from patient biopsies. We developed a decellularization protocol that combines the use of a Sterile milli Q water coupled with ionic detergent and DNase I. To date, most of the decellularization protocols currently used in oncological research relies on a linear development with long incubation times [50, 55, 56]. On the contrary, our approach involves a cyclic decellularization with short incubations in each solution. In this way, it is possible to identify with greater precision the number of cycles required for nuclear depletion, avoiding excessive loss of ECM components. In this study, paired normal mucosa and CRC tissues were decellularized employing sodium deoxycholate (SDC) as detergent. SDC is a ionic detergent frequently used throughout distinct decellularization protocols,

often in combination with several zwitterionic detergent due to its mild properties [41]. In literature, the majority of DET protocols uses sodium dodecylsulfate (SDS), a strong ionic agent, even though it has been proven that tends to disrupt native tissue structure, to remove GAG and to damage collagens [41]. Here, we proposed a DET protocol in which SDC and DNase I are able to remove more than 95 % of DNA content unchanging tissue composition and organization. Histological, immunohistochemical and ultrastructural evaluations confirmed the preservation of native tissue architecture and major ECM components (as laminin, collagen type IV and GAG). GAG preservation is crucial to maintain the biological activity of our patient-derived scaffolds. In fact, it has been demonstrated that GAG bind many growth factors and allow the specific and organized localization of ligands and associated proteins, such as mucins, complement, metalloproteases and their inhibitors, latent TGF-β, divers growth factors and chemokines [43]. As reported by others, GAG loss is an inevitable side effect of DET, because glycans are one of the most easily leachable component of the ECM and are also present in large amount on cell membranes that are totally removed along the DET process. Notably, in our study the loss of GAG is smaller compared with other similar studies [43]; moreover, the method we used for their quantification is not sensible to Hyaluronan, a glycan that is known to be excessive accumulated in breast [57], gastric [58] and colorectal [59] cancer tissues, probably underestimating the total concentration, especially in tumor samples, that in our hands seems more reliable with the histological readout. Through immunohistochemistry, qualitative evaluation of collagen distribution in (decellularized) normal vs tumor tissues showed, in agreement with the literature, a general increase in collagen deposition that consequently causes a tissue stiffness increment known as desmoplastic reaction [60]. At a first sight, in the decellularized samples, the quantification of collagens I to V seems to highlight their reduction in tumors compared with healthy mucosa. Based on these data we hypothized that the method used to solubilize collagen (pepsin incubation) fails to extract the total collagen amount, because in the pathological tissue it is strongly cross-linked with other

ECM components, especially with elastin [61]. Tumor ECM stiffening is caused, in part, by a raised activity of lysyl oxidase (LOX), the enzyme responsible for the cross-linking between collagen and elastin molecules [61]. Similarly to what found in other tumors, LOX was described to be upregulated in CRC comparing to normal colon and was shown to promote CRC progression [45]. This phenomenon was confirmed analyzing proteomic data of the collagen family peptides. We found that our decellularized CRC tissue possesses an increased content in COL1A1, COL1A2 and COL3A1 compared with healthy mucosa, as described by literature [62]. The occurrence of an active remodeling process in the analyzed DT samples was confirmed by the presence of MMP24. These data are in line with previous observations highlighting the CRC ability to deposit more dense and ordered collagen fibers in replacement of the proteolitically degraded normal stroma [63]. Decellularized normal colonic mucosa was characterized by the presence of several intracellular proteins, including vimentin, desmin, transgrelin and tropomyosin 2. A peculiar class of intracellular/membrane proteins found abundant in normal tissue is the protocadherins family (PCDH11Y, PCDHGC5, PCDH18). With respect to normal tissue, the cell-matrix adhesion proteins in cancer tissues were strongly down regulated, with the exception of protocadherin gamma C4 (PCDHGC4). Up to now, evidences of protocadherins involvement in cancer progression are very limited, but in general they act as tumor suppressor [64]; their down regulation in tumors increases cell proliferation and migration and some of them have been implied in the colorectal carcinogenesis [65]. In fact, adhesion molecules play a vital role in the induction and maintenance of tissue differentiation and their down-regulation has been previously implicated in CRC progression [66]. In the DT samples, the concomitant presence of high levels of endomucin (also known as Mucin-14), which is known to interfere with the assembly of focal adhesion complexes and to inhibit the interaction between cells and ECM, strongly evidence the tumor ability to regulate cell growth and differentiation.

A fundamental feature that a biologic-derived scaffold should possess is the ability to exert a biological activity even after deprivation of resident cells. From this point of view, we analyzed our decellularized samples demonstrating that, in addition to the architecture and the protein composition maintenance, also small molecules and soluble factors have been preserved with our decellularization protocol, conferring to the acellular ECM many of the biological properties already present in the native tissue. First, decellularized tumor samples have been shown to be more chemo-attractive than healthy samples against HT-29 cell line. This property is supported by the panel of peptides found more abundant in the tumor samples after proteomic analysis, some of which are related to immune system activation and regulation (EPX, PRG2, and DEFA3) and others directed involved in cell migration and motility, such as STOML2, HIF1α and TNS4 [48, 49, 67]. Secretoma analysis showed a marked increase of DEFA3 in tumor stroma compared to healthy counterpart. DEFA3 belong to the family of alpha-Defensin peptides and is part of the innate immune response active against a variety of bacteria, fungi, parasites and some viruses. DEFA3 is synthesized in neutrophil precursor cells, and mature circulating neutrophils release DEFA3 in inflammation areas. The gastrointestinal tract is a prominent site of DEFA3 secretion but recently a study described an elevated amount of DEFA1-3 in plasma and tumor tissue from patients with CRC and its correlation with prognosis and response to therapy in advanced CRC [68]. A study of Chavakis and colleagues demonstrated that the direct effect of DEFA is to induce apoptosis in endothelial cells, to inhibit endothelial cell adhesion and migration, exerting in general an anti-angiogenic effect [52]. After proteomic analysis, we confirmed the presence of this anti-angiogenic factor inside the decellularized tumor samples not only by ELISA and immunostaining, but especially by CAM assay that clearly demonstrated the less vessel attraction exerted by tumor matrix in respect to healthy tissue. This is an important finding since DEFA3, as indirect effector, is strongly related with inflammation and cancer. Indeed, neutrophils are prominent disease promoter, contributing to important steps during tumor progression

and metastasis [69]. Moreover, direct cancer-promoting effects were further demonstrated in a study where neutrophil extracellular traps (NETs), web-like structure in which chromatin and several proteins are externalized, were suggested to contribute to tumor relapse after surgery in patients with metastatic CRC [70]. Given that DEFA3 is one of the different class of proteins released in the microenvironment after neutrophil dead (known as NETosis or vital NETosis [71]), it is possible that contributes to the mechanism by which neutrophils increase tumor growth and progression. In literature, it has been shown that the release of neutrophils proteins into the inflamed tumor stroma is a strong activator of angiogenesis through stimulation of chemokine CXCL-8, also known as IL-8 [54]. In addition, a recent research work showed that released DEFA proteins are able to induce the secretion of IL-8 in HT-29 cell line through the activation of ERK1/2 signaling pathway [53]. Also in our hand, HT-29 cells were able to over-expressed *IL-8* transcript after conditioning with either exogenous or decellularized matrix-related DEFA3, but this increase in gene expression was statistically different between acellular tumor and healthy mucosa samples only when the cell line was cultivated in 3D biologic-derived environment. This finding highlights the importance of architecture and spatial (and maybe temporal) availability of peptides and factors retained by the scaffold, and strongly supports the idea that acellular matrix obtained *via* decellularization resembles the original microenvironment. Therefore, this approach could be very useful in improving *in vitro* pre-clinical studies given that mimics more effectively the *in vivo* environment than conventional 2D cultures. Indeed, decellularized ECM allows cell growth and adaptation to a rich protein milieu respecting their timing, mechanical, and biological signal requirement. Moreover, it would also allow reducing *in vivo* xenogeneic tests, becoming not strictly necessary having the ability to recreate *in vitro* a reliable tissue-like structure. More experiments needed to confirm our results and to deeper investigate ECM biological properties relating the presence of diverse peptides to different tumor conditions such as CRC stages or aggressiveness and therapy resistance.

# CONCLUSIONS

With this thesis, we demonstrated that detergent enzymatic treatment is a good decellularization method to obtain acellular scaffold from both healthy and tumor biopsies. Our protocol allows preserving original structure, ultrastructure, architecture, and protein composition. Moreover, peptides and small molecules retained in the decellularized matrices maintained biological activity and effect, nominating this technique an interesting approach to overcome obsolete 2D culture models and to perform more relevant *in vitro* 3D clinical screening and drug delivery assays.

# FUTURE PERSPECTIVE

The present work allowed us to produce a scientific paper currently submitted to the peer-review journal “European Journal of Cancer”. Based on these encouraging results we have decided to apply this approach to the study of the metastatic CRC (mCRC) environment. Liver is the most common site for CRC metastasis: about 50% of CRC patients develop liver metastases during the disease progression and in 15-25% of patients it is already present at diagnosis. In addition, the highest mortality rate in this disease is in the case of mCRC. The experimental results of this thesis have shown how the decellularization protocol is an effective method for producing acellular scaffolds that allow us to study the influence of the non-cellular component of the tumor niche.

In the light of these promising results, the laboratory in which I carried out this project established a scientific collaboration with the Foundation For Liver Research - Institute of Hepatology (Denmark hill campus of King’s College of London). The future objective is to study the tumor microenvironment of liver metastasis niche derived from primitive CRC. In this project, in addition to standardizing a new decellularization protocol, we are going to study the proteome and secretome profile of the mCRC in comparison with

healthy liver and with primitive CRC. In addition, CRC liver metastasis will be repopulated with primary CRC cells to perform pharmacological treatment tests and consequently evaluate the response to treatment in the acellular patients-derived 3D environment in comparison with conventional 2D plate.

# REFERENCES


1. **Siegel RL, Miller KD, Jemal A: Cancer Statistics, 2017. *CA: a cancer journal for clinicians* 2017, 67(1):7-30.**
2. **Siegel RL, Miller KD, Fedewa SA, Ahnen DJ, Meester RGS, Barzi A, Jemal A: Colorectal cancer statistics, 2017. *CA: a cancer journal for clinicians* 2017, 67(3):177-193.**
3. **Bishehsari F, Mahdavinia M, Vacca M, Malekzadeh R, Mariani-Costantini R: Epidemiological transition of colorectal cancer in developing countries: Environmental factors, molecular pathways, and opportunities for prevention. *World J Gastroentero* 2014, 20(20):6055-6072.**
4. **Fearon ER, Vogelstein B: A genetic model for colorectal tumorigenesis. *Cell* 1990, 61(5):759-767.**
5. **Jasperson KW, Tuohy TM, Neklason DW, Burt RW: Hereditary and Familial Colon Cancer. *Gastroenterology* 2010, 138(6):2044-2058.**
6. **Grady WM, Carethers JM: Genomic and epigenetic instability in colorectal cancer pathogenesis. *Gastroenterology* 2008, 135(4):1079-1099.**
7. **Leslie Sobin MG, Christian Wittekind: TNM Classification of Malignant Tumours, 7th Edition citation: Wiley-Blackwell; 2009.**
8. **Phipps AI, Limburg PJ, Baron JA, Burnett-Hartman AN, Weisenberger DJ, Laird PW, Sinicrope FA, Rosty C, Buchanan DD, Potter JD *et al*: Association Between Molecular Subtypes of Colorectal Cancer and Patient Survival. *Gastroenterology* 2015, 148(1):77-U498.**
9. **Hanahan D, Weinberg RA: The hallmarks of cancer. *Cell* 2000, 100(1):57-70.**
10. **Hanahan D, Weinberg RA: Hallmarks of Cancer: The Next Generation. *Cell* 2011, 144(5):646-674.**
11. **Hanahan D, Coussens LM: Accessories to the Crime: Functions of Cells Recruited to the Tumor Microenvironment. *Cancer Cell* 2012, 21(3):309-322.**
12. **Pietras K, Ostman A: Hallmarks of cancer: Interactions with the tumor stroma. *Experimental cell research* 2010, 316(8):1324-1331.**
13. **Pietras K, Ostman A: Hallmarks of cancer: interactions with the tumor stroma. *Experimental cell research* 2010, 316(8):1324-1331.**
14. **Lu P, Weaver VM, Werb Z: The extracellular matrix: a dynamic niche in cancer progression. *The Journal of cell biology* 2012, 196(4):395-406.**
15. **Hinderer S, Layland SL, Schenke-Layland K: ECM and ECM-like materials — Biomaterials for applications in regenerative medicine and cancer therapy. *Advanced Drug Delivery Reviews* 2016, 97(Supplement C):260-269.**
16. **Levental KR, Yu HM, Kass L, Lakins JN, Egeblad M, Erler JT, Fong SFT, Csiszar K, Giaccia A, Weninger W *et al*: Matrix Crosslinking Forces Tumor Progression by Enhancing Integrin Signaling. *Cell* 2009, 139(5):891-906.**
17. **Pandol S, Edderkaoui M, Gukovsky I, Lugea A, Gukovskaya A: Desmoplasia of Pancreatic Ductal Adenocarcinoma. *Clin Gastroenterol H* 2009, 7(11):S44-S47.**
18. **Erler JT, Bennewith KL, Nicolau M, Dornhofer N, Kong C, Le QT, Chi JTA, Jeffrey SS, Giaccia AJ: Lysyl oxidase is essential for hypoxia-induced metastasis. *Nature* 2006, 440(7088):1222-1226.**

19. **Slattery ML, John E, Torres-Mejia G, Stern M, Lundgreen A, Hines L, Giuliano A, Baumgartner K, Herrick J, Wolff RK: Matrix Metalloproteinase Genes Are Associated with Breast Cancer Risk and Survival: The Breast Cancer Health Disparities Study.** ***Plos One*** **2013, 8(5).**
20. **Sorensen HT, Friis S, Olsen JH, Thulstrup AM, Mellemkjaer L, Linet M, Trichopoulos D, Vilstrup H, Olsen J: Risk of liver and other types of cancer in patients with cirrhosis: a nationwide cohort study in Denmark.** ***Hepatology*** **1998, 28(4):921-925.**
21. **Neglia JP, Fitzsimmons SC, Maisonneuve P, Schoni MH, Schoniaffolter F, Corey M, Lowenfels AB, Boyle P, Dozor AJ, Durie P: The Risk of Cancer among Patients with Cystic-Fibrosis.** ***New Engl J Med*** **1995, 332(8):494-499.**
22. **Boyd NF, Guo H, Martin LJ, Sun LM, Stone J, Fishell E, Jong RA, Hislop G, Chiarelli A, Minkin S** ***et al*****: Mammographic density and the risk and detection of breast cancer.** ***New Engl J Med*** **2007, 356(3):227-236.**
23. **Fessler E, Medema JP: Colorectal Cancer Subtypes: Developmental Origin and Microenvironmental Regulation.** ***Trends in cancer*** **2016, 2(9):505-518.**
24. **Alemany-Ribes M, Semino CE: Bioengineering 3D environments for cancer models.** ***Adv Drug Deliv Rev*** **2014, 79-80:40-49.**
25. **Xu X, Farach-Carson MC, Jia X: Three-dimensional in vitro tumor models for cancer research and drug evaluation.** ***Biotechnology advances*** **2014, 32(7):1256-1268.**
26. **Sutherland RM, McCredie JA, Inch WR: Growth of multicell spheroids in tissue culture as a model of nodular carcinomas.** ***Journal of the National Cancer Institute*** **1971, 46(1):113-120.**
27. **Friedrich J, Ebner R, Kunz-Schughart LA: Experimental anti-tumor therapy in 3-D: spheroids--old hat or new challenge?** ***International journal of radiation biology*** **2007, 83(11-12):849-871.**
28. **Soranzo C, Della Torre G, Ingrosso A: Formation, growth and morphology of multicellular tumor spheroids from a human colon carcinoma cell line (LoVo).** ***Tumori*** **1986, 72(5):459-467.**
29. **Lees RK, Sordat B, MacDonald HR: Multicellular tumor spheroids of human colon carcinoma origin. Kinetic analysis of infiltration and in situ destruction in a xenogeneic (murine) host.** ***Experimental cell biology*** **1981, 49(4):207-219.**
30. **Lange CS, Djordjevic B, Brock WA: The hybrid spheroid clonogenic assay for the intrinsic radio- and chemo-sensitivities of human tumors.** ***International journal of radiation oncology, biology, physics*** **1992, 24(3):511-517.**
31. **Mellor HR, Ferguson DJ, Callaghan R: A model of quiescent tumour microregions for evaluating multicellular resistance to chemotherapeutic drugs.** ***British journal of cancer*** **2005, 93(3):302-309.**
32. **Weiswald LB, Richon S, Validire P, Briffod M, Lai-Kuen R, Cordelieres FP, Bertrand F, Dargere D, Massonnet G, Marangoni E** ***et al*****: Newly characterised ex vivo colospheres as a three-dimensional colon cancer cell model of tumour aggressiveness.** ***British journal of cancer*** **2009, 101(3):473-482.**
33. **Chen Y, Gao D, Liu H, Lin S, Jiang Y: Drug cytotoxicity and signaling pathway analysis with three-dimensional tumor spheroids in a microwell-based microfluidic chip for drug screening.** ***Analytica chimica acta*** **2015, 898:85-92.**

34. **Lee KY, Mooney DJ: Hydrogels for tissue engineering. *Chem Rev* 2001, 101(7):1869-1879.**
35. **Pampaloni F, Reynaud EG, Stelzer EH: The third dimension bridges the gap between cell culture and live tissue. *Nature reviews Molecular cell biology* 2007, 8(10):839-845.**
36. **Gill BJ, West JL: Modeling the tumor extracellular matrix: Tissue engineering tools repurposed towards new frontiers in cancer biology. *Journal of biomechanics* 2014, 47(9):1969-1978.**
37. **Infanger DW, Lynch ME, Fischbach C: Engineered Culture Models for Studies of Tumor-Microenvironment Interactions. *Annu Rev Biomed Eng* 2013, 15:29-53.**
38. **Schmeichel KL, Bissell MJ: Modeling tissue-specific signaling and organ function in three dimensions. *J Cell Sci* 2003, 116(12):2377-2388.**
39. **Gill BJ, Gibbons DL, Roudsari LC, Saik JE, Rizvi ZH, Roybal JD, Kurie JM, West JL: A Synthetic Matrix with Independently Tunable Biochemistry and Mechanical Properties to Study Epithelial Morphogenesis and EMT in a Lung Adenocarcinoma Model. *Cancer research* 2012, 72(22):6013-6023.**
40. **Badylak SF, Taylor D, Uygun K: Whole-Organ Tissue Engineering: Decellularization and Recellularization of Three-Dimensional Matrix Scaffolds. *Annual Review of Biomedical Engineering, Vol 13* 2011, 13:27-53.**
41. **Gilbert TW, Sellaro TL, Badylak SF: Decellularization of tissues and organs. *Biomaterials* 2006, 27(19):3675-3683.**
42. **Genovese L, Zawada L, Tosoni A, Ferri A, Zerbi P, Allevi R, Nebuloni M, Alfano M: Cellular Localization, Invasion, and Turnover Are Differently Influenced by Healthy and Tumor-Derived Extracellular Matrix. *Tissue Eng Pt A* 2014, 20(13-14):2005-2018.**
43. **Pinto ML, Rios E, Silva AC, Neves SC, Caires HR, Pinto AT, Duraes C, Carvalho FA, Cardoso AP, Santos NC *et al*: Decellularized human colorectal cancer matrices polarize macrophages towards an anti-inflammatory phenotype promoting cancer cell invasion via CCL18. *Biomaterials* 2017, 124:211-224.**
44. **Ponce ML, Kleinmann HK: The chick chorioallantoic membrane as an in vivo angiogenesis model. *Current protocols in cell biology* 2003, Chapter 19:Unit 19 15.**
45. **Baker AM, Bird D, Lang G, Cox TR, Erler JT: Lysyl oxidase enzymatic function increases stiffness to drive colorectal cancer progression through FAK. *Oncogene* 2013, 32(14):1863-1868.**
46. **Nebuloni M, Albarello L, Andolfo A, Magagnotti C, Genovese L, Locatelli I, Tonon G, Longhi E, Zerbi P, Allevi R *et al*: Insight On Colorectal Carcinoma Infiltration by Studying Perilesional Extracellular Matrix. *Scientific reports* 2016, 6:22522.**
47. **Pankova D, Chen Y, Terajima M, Schliekelman MJ, Baird BN, Fahrenholtz M, Sun L, Gill BJ, Vadakkan TJ, Kim MP *et al*: Cancer-Associated Fibroblasts Induce a Collagen Cross-link Switch in Tumor Stroma. *Molecular cancer research : MCR* 2016, 14(3):287-295.**
48. **Muharram G, Sahgal P, Korpela T, De Franceschi N, Kaukonen R, Clark K, Tulasne D, Carpen O, Ivaska J: Tensin-4-dependent MET stabilization is essential for survival and proliferation in carcinoma cells. *Developmental cell* 2014, 29(4):421-436.**

**49.** **Song L, Liu L, Wu Z, Lin C, Dai T, Yu C, Wang X, Wu J, Li M, Li J: Knockdown of stomatin-like protein 2 (STOML2) reduces the invasive ability of glioma cells through inhibition of the NF-kappaB/MMP-9 pathway.** ***The Journal of pathology*** **2012, 226(3):534-543.**

**50.** **Dunne LW, Huang Z, Meng W, Fan X, Zhang N, Zhang Q, An Z: Human decellularized adipose tissue scaffold as a model for breast cancer cell growth and drug treatments.** ***Biomaterials*** **2014, 35(18):4940-4949.**

**51.** **Stratmann AT, Fecher D, Wangorsch G, Gottlich C, Walles T, Walles H, Dandekar T, Dandekar G, Nietzer SL: Establishment of a human 3D lung cancer model based on a biological tissue matrix combined with a Boolean in silico model.** ***Molecular oncology*** **2014, 8(2):351-365.**

**52.** **Chavakis T, Keiper T, Matz-Westphal R, Hersemeyer K, Sachs UJ, Nawroth PP, Preissner KT, Santoso S: The junctional adhesion molecule-C promotes neutrophil transendothelial migration in vitro and in vivo.** ***The Journal of biological chemistry*** **2004, 279(53):55602-55608.**

**53.** **Ibusuki K, Sakiyama T, Kanmura S, Maeda T, Iwashita Y, Nasu Y, Sasaki F, Taguchi H, Hashimoto S, Numata M** ***et al*****: Human neutrophil peptides induce interleukin-8 in intestinal epithelial cells through the P2 receptor and ERK1/2 signaling pathways.** ***International journal of molecular medicine*** **2015, 35(6):1603-1609.**

**54.** **Khine AA, Del Sorbo L, Vaschetto R, Voglis S, Tullis E, Slutsky AS, Downey GP, Zhang H: Human neutrophil peptides induce interleukin-8 production through the P2Y6 signaling pathway.** ***Blood*** **2006, 107(7):2936-2942.**

**55.** **Chen HJ, Wei Z, Sun J, Bhattacharya A, Savage DJ, Serda R, Mackeyev Y, Curley SA, Bu P, Wang L** ***et al*****: A recellularized human colon model identifies cancer driver genes.** ***Nature biotechnology*** **2016, 34(8):845-851.**

**56.** **Genovese L, Zawada L, Tosoni A, Ferri A, Zerbi P, Allevi R, Nebuloni M, Alfano M: Cellular localization, invasion, and turnover are differently influenced by healthy and tumor-derived extracellular matrix.** ***Tissue engineering Part A*** **2014, 20(13-14):2005-2018.**

**57.** **Auvinen P, Tammi R, Parkkinen J, Tammi M, Agren U, Johansson R, Hirvikoski P, Eskelinen M, Kosma VM: Hyaluronan in peritumoral stroma and malignant cells associates with breast cancer spreading and predicts survival.** ***The American journal of pathology*** **2000, 156(2):529-536.**

**58.** **Setala LP, Tammi MI, Tammi RH, Eskelinen MJ, Lipponen PK, Agren UM, Parkkinen J, Alhava EM, Kosma VM: Hyaluronan expression in gastric cancer cells is associated with local and nodal spread and reduced survival rate.** ***British journal of cancer*** **1999, 79(7-8):1133-1138.**

**59.** **Kobel M, Weichert W, Cruwell K, Schmitt WD, Lautenschlager C, Hauptmann S: Epithelial hyaluronic acid and CD44v6 are mutually involved in invasion of colorectal adenocarcinomas and linked to patient prognosis.** ***Virchows Archiv : an international journal of pathology*** **2004, 445(5):456-464.**

**60.** **Crotti S, Piccoli M, Rizzolio F, Giordano A, Nitti D, Agostini M: Extracellular Matrix and Colorectal Cancer: How Surrounding Microenvironment Affects Cancer Cell Behavior?** ***Journal of cellular physiology*** **2017, 232(5):967-975.**

**61.** **Cox TR, Gartland A, Erler JT: Lysyl Oxidase, a Targetable Secreted Molecule Involved in Cancer Metastasis.** ***Cancer research*** **2016, 76(2):188-192.**

62. **Zou X, Feng B, Dong T, Yan G, Tan B, Shen H, Huang A, Zhang X, Zhang M, Yang P *et al*: Up-regulation of type I collagen during tumorigenesis of colorectal cancer revealed by quantitative proteomic analysis. *Journal of proteomics* 2013, 94:473-485.**
63. **Birk JW, Tadros M, Moezardalan K, Nadyarnykh O, Forouhar F, Anderson J, Campagnola P: Second harmonic generation imaging distinguishes both high-grade dysplasia and cancer from normal colonic mucosa. *Digestive diseases and sciences* 2014, 59(7):1529-1534.**
64. **Berx G, van Roy F: Involvement of members of the cadherin superfamily in cancer. *Cold Spring Harbor perspectives in biology* 2009, 1(6):a003129.**
65. **Losi L, Parenti S, Ferrarini F, Rivasi F, Gavioli M, Natalini G, Ferrari S, Grande A: Down-regulation of mu-protocadherin expression is a common event in colorectal carcinogenesis. *Human pathology* 2011, 42(7):960-971.**
66. **Nigam AK, Savage FJ, Boulos PB, Stamp GW, Liu D, Pignatelli M: Loss of cell-cell and cell-matrix adhesion molecules in colorectal cancer. *British journal of cancer* 1993, 68(3):507-514.**
67. **Nagaraju GP, Bramhachari PV, Raghu G, El-Rayes BF: Hypoxia inducible factor-1alpha: Its role in colorectal carcinogenesis and metastasis. *Cancer letters* 2015, 366(1):11-18.**
68. **Albrethsen J, Moller CH, Olsen J, Raskov H, Gammeltoft S: Human neutrophil peptides 1, 2 and 3 are biochemical markers for metastatic colorectal cancer. *European journal of cancer* 2006, 42(17):3057-3064.**
69. **Gregory AD, Houghton AM: Tumor-associated neutrophils: new targets for cancer therapy. *Cancer research* 2011, 71(7):2411-2416.**
70. **Tohme S, Yazdani HO, Al-Khafaji AB, Chidi AP, Loughran P, Mowen K, Wang Y, Simmons RL, Huang H, Tsung A: Neutrophil Extracellular Traps Promote the Development and Progression of Liver Metastases after Surgical Stress. *Cancer research* 2016, 76(6):1367-1380.**
71. **Jorch SK, Kubes P: An emerging role for neutrophil extracellular traps in noninfectious disease. *Nature medicine* 2017, 23(3):279-287.**